Supplemental Information

Sindrilaru et al. 'An unrestrained inflammatory M1 macrophage population induced by iron impairs wound healing in humans and mice

Supplemental Figure 1 Macrophages accumulate in CVU. (**A**) Immunohistochemistry staining for the macrophage specific marker CD68 on paraffin-embedded tissue taken from AW of healthy donors 1 and 2 days after wounding and from patients with non-healing CVU. Scale bars indicate 100μm. The dashed line indicates the junction between epidermis (e) and wound margin (wm). (**B**) Flow-cytometry analysis of wound macrophages purified from tissue of acute wounds (AW) at day 2 and day 5 after wounding and CVU gated according to SSC and CD68.

Supplemental Figure 2 Injection of recombinant TNFα in the margins of acute wounds results in impaired wound healing in mice. Standardized excisional wounds were inflicted as described in the Methods section (Supplemental information online). Statistical analysis of 20 wound areas per experimental group were quantified at days 3, 5, 7 and 10 after wounding and expressed as percentage of the initial (day 0) wound size for mice treated with rTNFα or PBS. Results were given as mean ± SD (n=5) and reflect 1 of 2 independent experiments. *$P < 0.05$, **$P < 0.01$ by Mann-Whitney test.

Supplemental Figure 3 (A) Representative photomicrographs with double immunostaining of skin cryosections from iron-loaded mice on day 2 and day 5 after wounding for M1 and M2 macrophage activation markers TNFα (red), CD206 (green) (upper panel), IL-12 (red) and Arginase-1 (green) (lower panel). DAPI stained cell nuclei (blue). (scale bar 150μm; dashed

line indicates the junction between eschar (es) and wound margin (wm). **(B)** Pro-inflammatory activation of macrophages in wound margins of iron-dextran loaded mice. Western blot analysis was performed with tissue lysates of normal skin and of wound margins on day 2 and day 5 after wounding taken from iron-dextran and PBS-dextran treated mice. Representative Western blot showing increased expression of the M1 macrophage activation markers TNFα and CCR2 in iron-dextran treated wounds when compared to PBS-dextran control wounds at days 2 and 5 after wounding. TNFα and CCR2 were not expressed in normal skin of the two experimental groups. Actin served as loading control.

Supplemental Figure 4 Redox-active iron reproduces the CVU macrophage activation phenotype *in vitro*. Flow-cytometry analysis of macrophages derived from peripheral blood mononuclear cells were exposed to Fe(III)-chloride/ascorbate and H_2O_2 *in vitro* (closed black bars) mimicking the Fenton reaction in CVU *in vivo*. Treatment with IFNγ and LPS resulted in polarization of macrophages to M1 activation (IFNγ+LPS Mϕ) (closed grey bars). Alternatively, incubation with IL-4 and Dexamethasone resulted in M2 polarized macrophages (Dex + IL-4 Mϕ) (open bars). Striped bars represent mature untreated Mϕ (resting Mϕ). Results were given as bar diagrams in RFU (Relative Fluorescence Units) as detailed in the Methods section. Results are representative for 5 different PBMC-derived macrophage preparations.

Supplemental Figure 5 Iron overload resulted in persistent accumulation of macrophages and delayed wound healing in mice. **(A)** Statistical analysis of 20 wound areas per experimental group quantified at days 0, 2, 3, 5, 7 and 10 after wounding and expressed as percentage of the initial (day 0) wound size for mice treated with iron-dextran or PBS-dextran. Results were given as mean ± SD (n=5) and reflect 1 of 2 independent experiments. $*P < 0.05$, $**P < 0.01$ by Mann-Whitney test. **(B)** Numbers of $F4/80^+$ infiltrating macrophages in wound margins

from PBS-dextran and iron-dextran treated mice at days 1, 2, 3, 4 and 5 after wounding were counted for 8 different wounds per experimental group and time point in 5 HPF/sample. Results were given as mean ratio of F4/80$^+$ cells of total cell numbers counted in the dermis. Bars indicate the mean ± SD (n=8), $^{**}p < 0.01$ by Student's *t* test.

Supplemental Figure 6 (**A**) Selective depletion of macrophages in wound margins following injection of clodronate liposomes. Clodronate liposomes or control PBS liposomes were injected around the wounds of iron-dextran treated and PBS-dextran treated control mice at day 4 after wounding at a dose of 12.5mg/100µl/wound. Wound margins taken 24h after clodronate or PBS liposomes injection were stained with anti-mouse F4/80-Alexa®488 for macrophages (green). An almost complete depletion of F4/80 positive macrophages from wounds treated with clodronate liposomes was observed when compared to wounds treated with PBS-control liposomes. Cryosections derived from iron-treated mice 24h after injection of clodronate liposomes or PBS-control liposomes were stained with anti-mouse CD205-Alexa®488 for dendritic cells (**B**), anti-mouse CD207-Alexa®488 (Langerin) for Langerhans cells (**C**), anti-mouse GR-1-Alexa®488 for granulocytes (**D**), CD117-Alexa®488 for mast cells (**E**) and with anti-mouse CD4-Alexa®488 for helper T lymphocytes (**F**) and anti-mouse CD8-Alexa®488 for cytotoxic T lymphocytes (**G**) (green). Cell nuclei were counterstained with DAPI (blue) (scale bar indicates 150 µm; the dashed line indicates the junction between eschar and wound margin; es, eschar; wm, wound margin). Quantitative analysis and comparison of the inflammatory infiltrate was performed by counting cells staining positive for F4/80 (**A**), CD205 (**B**), Langerin (**C**), GR-1 (**D**), CD3 (**E**) and CD117 (**F**) in wound margins of iron-dextran treated mice 24h after injection of clodronate liposomes or PBS control liposomes. Results were given as mean ratio of positive counts of total nuclei counted in 5 high power fields per 4 different wounds ($n = 4$); $^{**}p < 0.01$ by Student's *t* test.'

Supplemental Figure 7 Accumulation of hydroxyl radicals in wound margins of full thickness excisional wounds in iron-dextran loaded mice. Representative photomicrographs of fresh wound cryosections from iron-loaded mice compared with PBS-dextran-treated control mice (**A**) and with iron-loaded mice treated with etanercept (**B**). Oxidative burst was assessed in wound margins by incubation of cryosections with DHR alone or with the H_2O_2 scavenger catalase (Cat) or the $OH^{\cdot}$ quenching DMSO. (scale bar indicates 50μm; the dashed line indicates the junction between epidermis and dermis; e, epidermis; es, eschar; wm, wound margin). Representative photomicrographs of 5 different wounds analyzed in 3 independent experiments.

Supplemental Figure 8 Enhanced protein carbonylation in CVU margins. Oxyblot analysis of tissue lysates from CVU and normal skin (NS) of the patients' same legs. Positive bands indicate increased protein carbonylation of CVU compared to NS tissue lysates. A 50kDa protein (arrow) persistently occurred in all studied CVU lysates. Mixtures of carbonylated proteins of known molecular weight served as positive controls (STD). Actin served as loading control.

Supplemental Figure 9 Western blot of CVU and NS tissue lysates equilibrated to total actin showing high expression of γH2AX in CVU margin, but not in NS of the same patients' legs (n=3).

Supplemental Table 1.
Characterization of studied patients with chronic venous leg ulcers

Patient No.	Age	Gender	Persistence of ulcer before treatment (months)	Conventional therapy[a] (months)
1	65	male	5	5
2	68	female	8	6
3	58	female	6	6
4	71	female	9	7
5	70	male	8	7
6	78	female	11	6
7	63	male	6	6
8	68	female	7	6
9	61	female	10	8
10	60	male	7	7
11	82	female	12	8
12	77	female	6	5
13	78	female	8	5
14	68	male	7	6
15	71	female	7	6
16	65	male	9	7

a Compression therapy and modern wound management without application of growth factors

Supplemental Figure 1

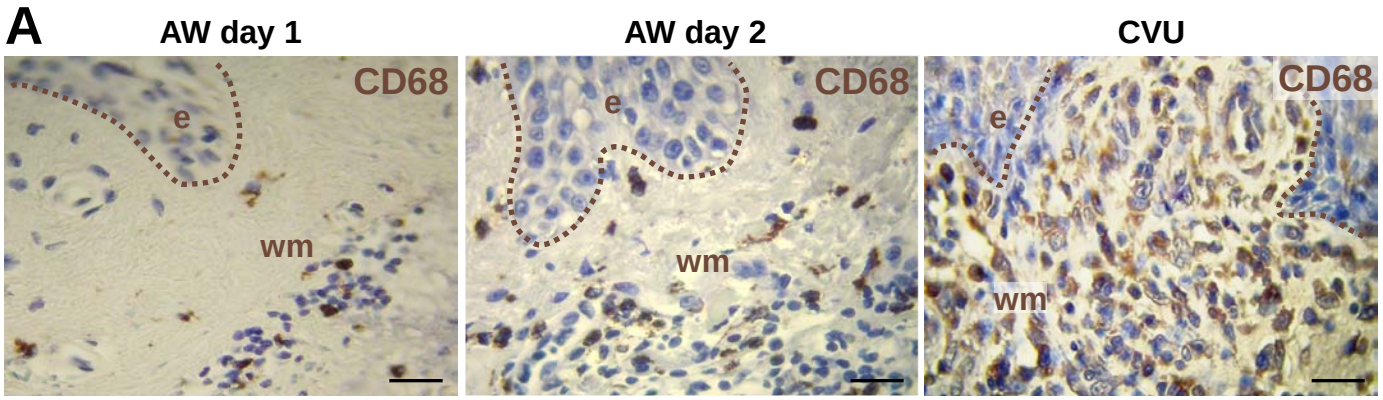

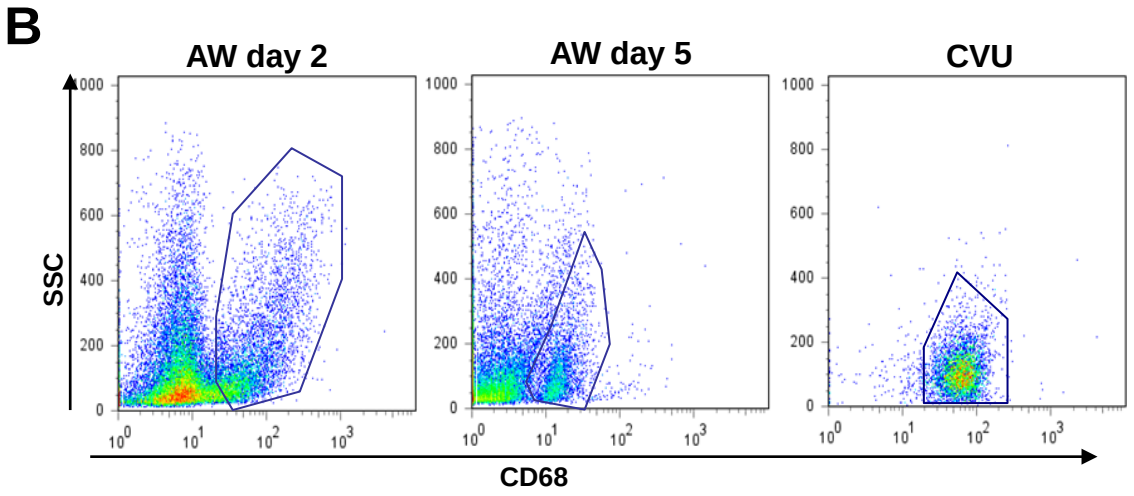

Supplemental Figure 2

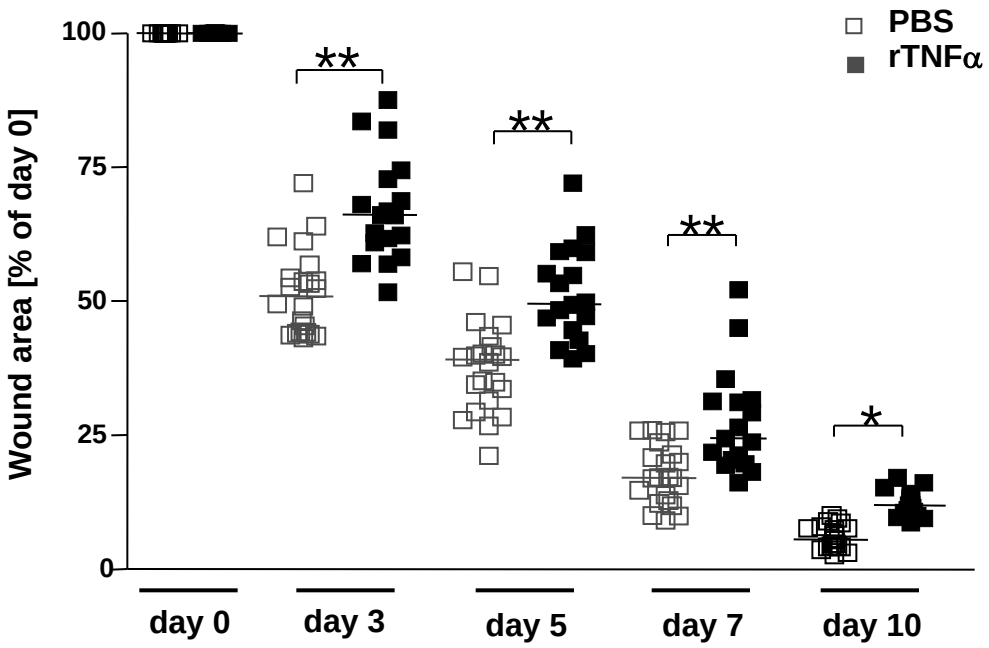

Supplemental Figure 3

A

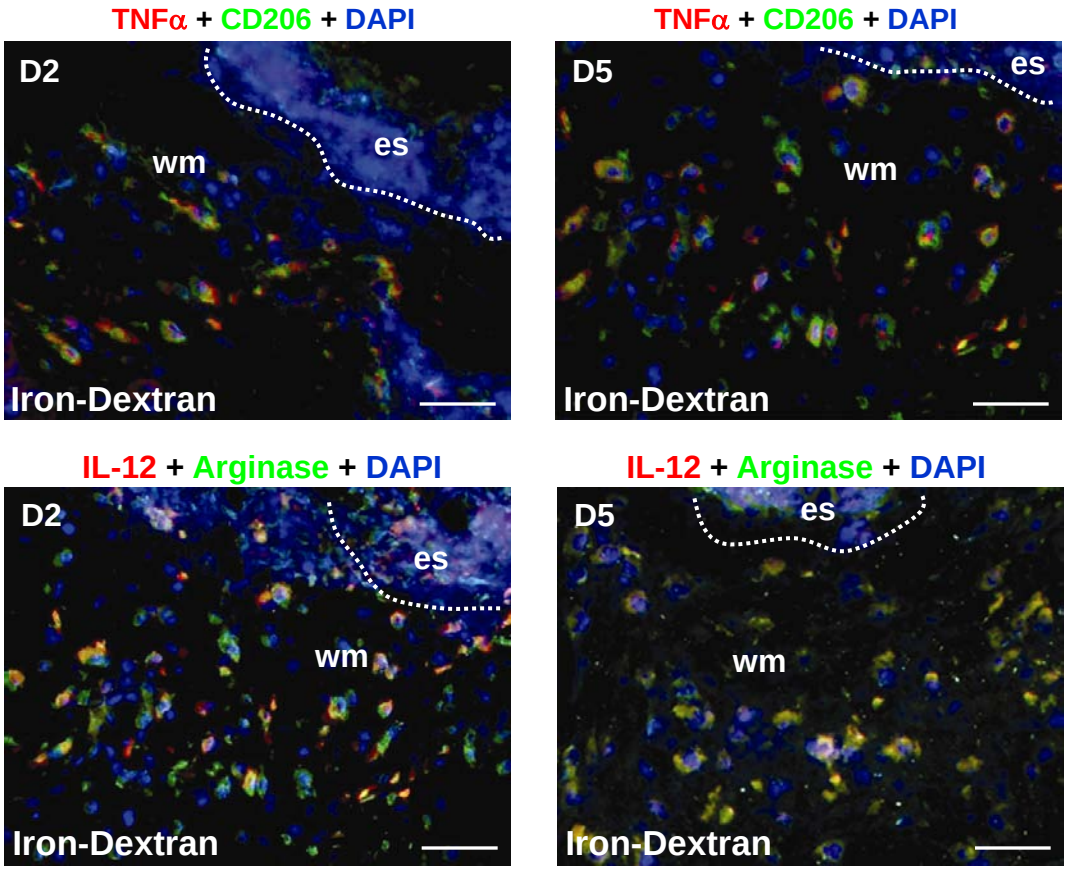

B

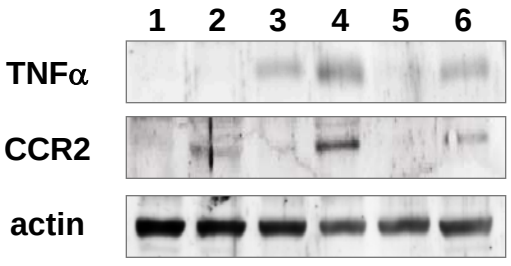

1 PBS-dextran treated mice normal skin
2 Iron-dextran treated mice normal skin
3 PBS-dextran treated mice day 2 after wounding
4 Iron-dextran treated mice day 2 after wounding
5 PBS-dextran treated mice day 5 after wounding
6 Iron-dextran treated mice day 5 after wounding

Supplemental Figure 4

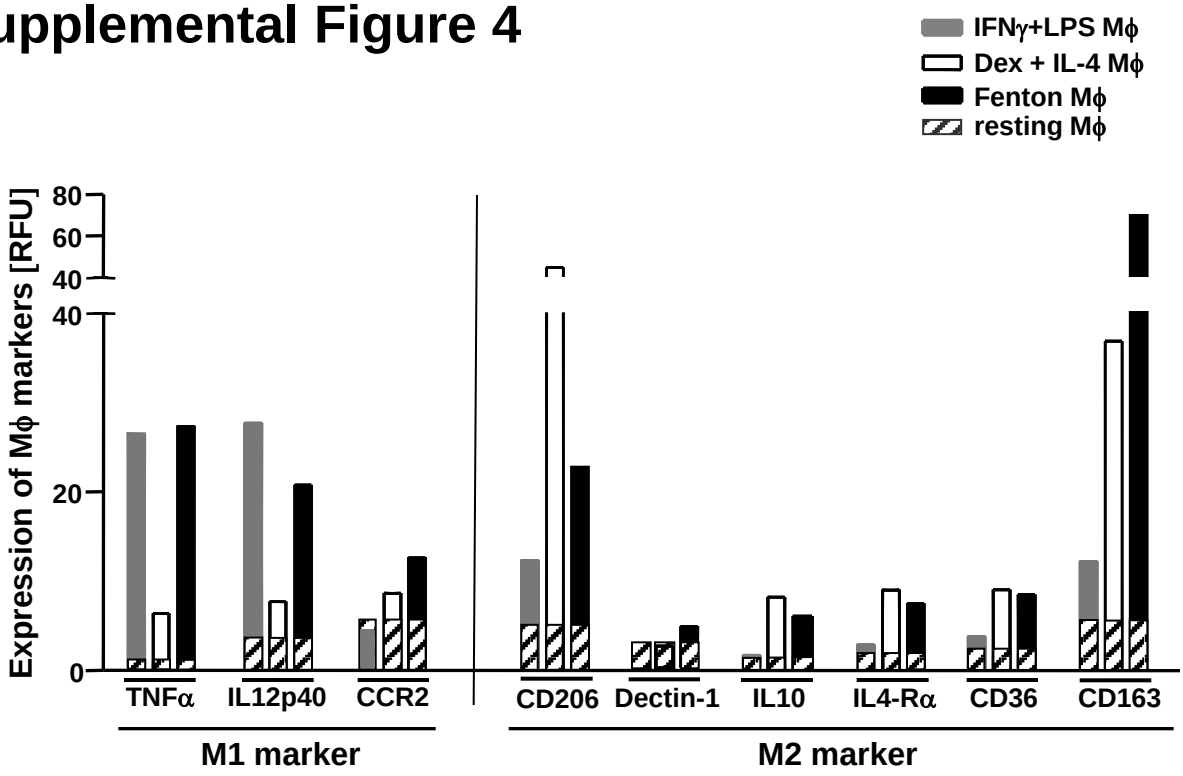

Supplemental Figure 5

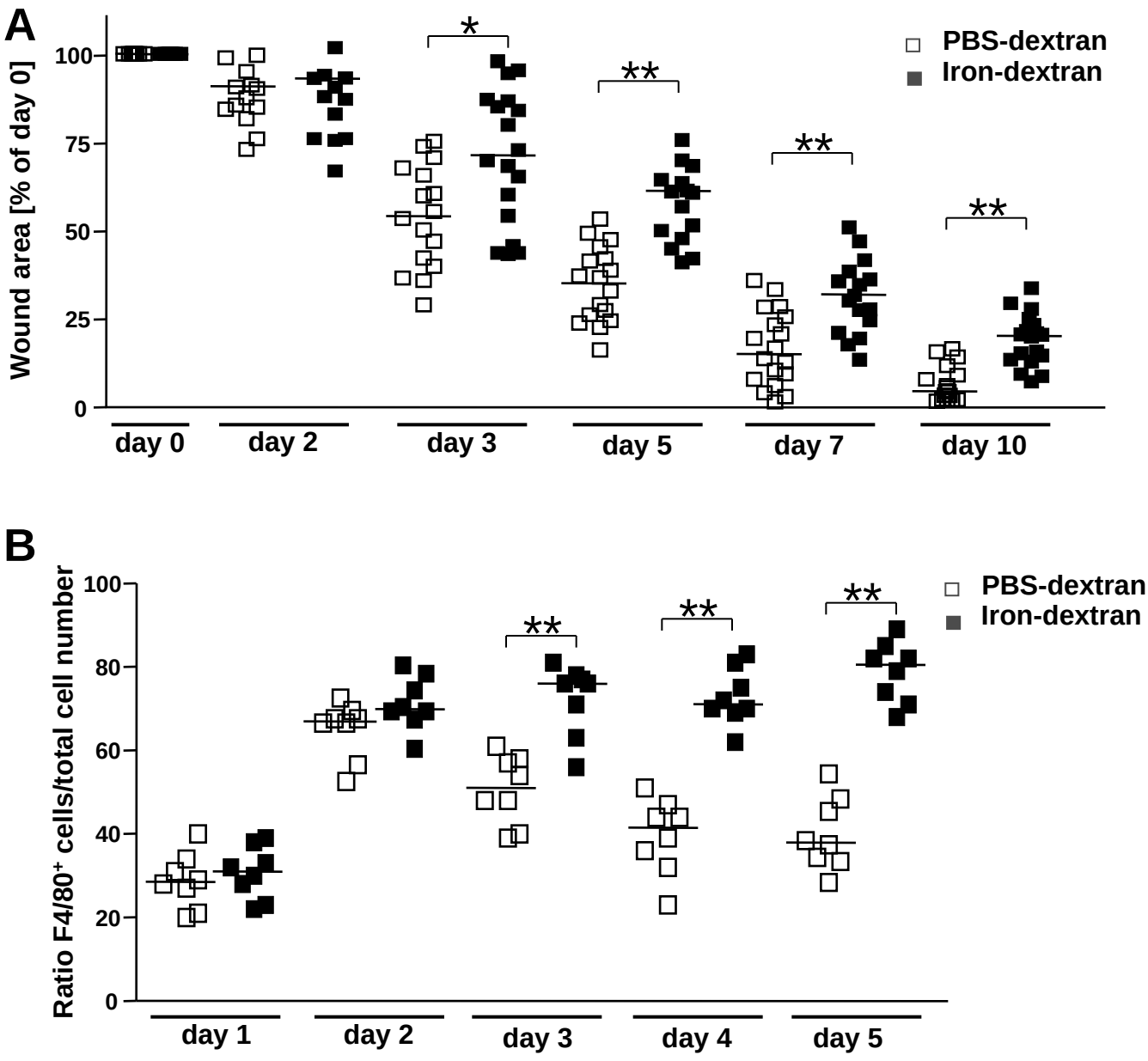

Supplemental Figure 6

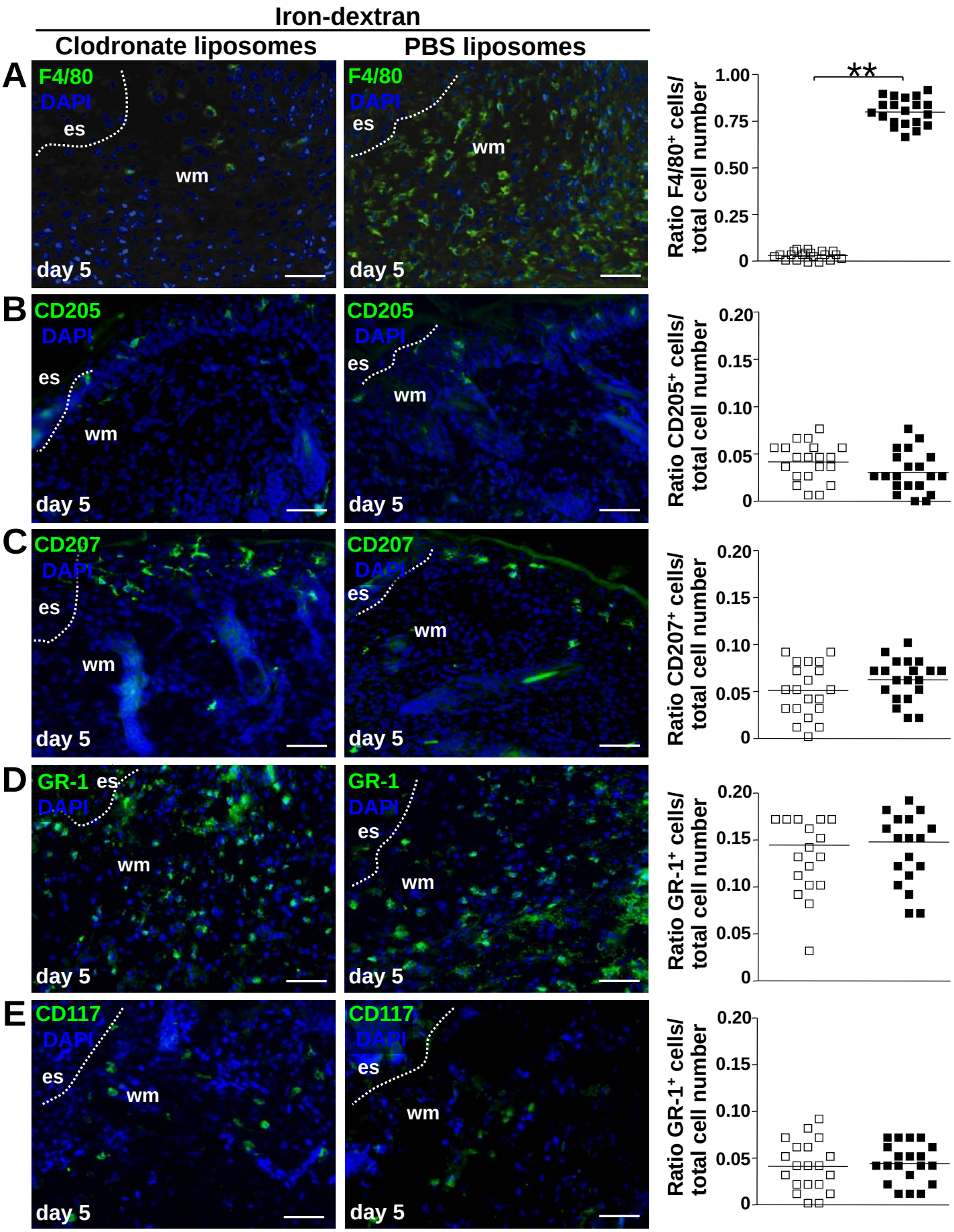

Supplemental Figure 6

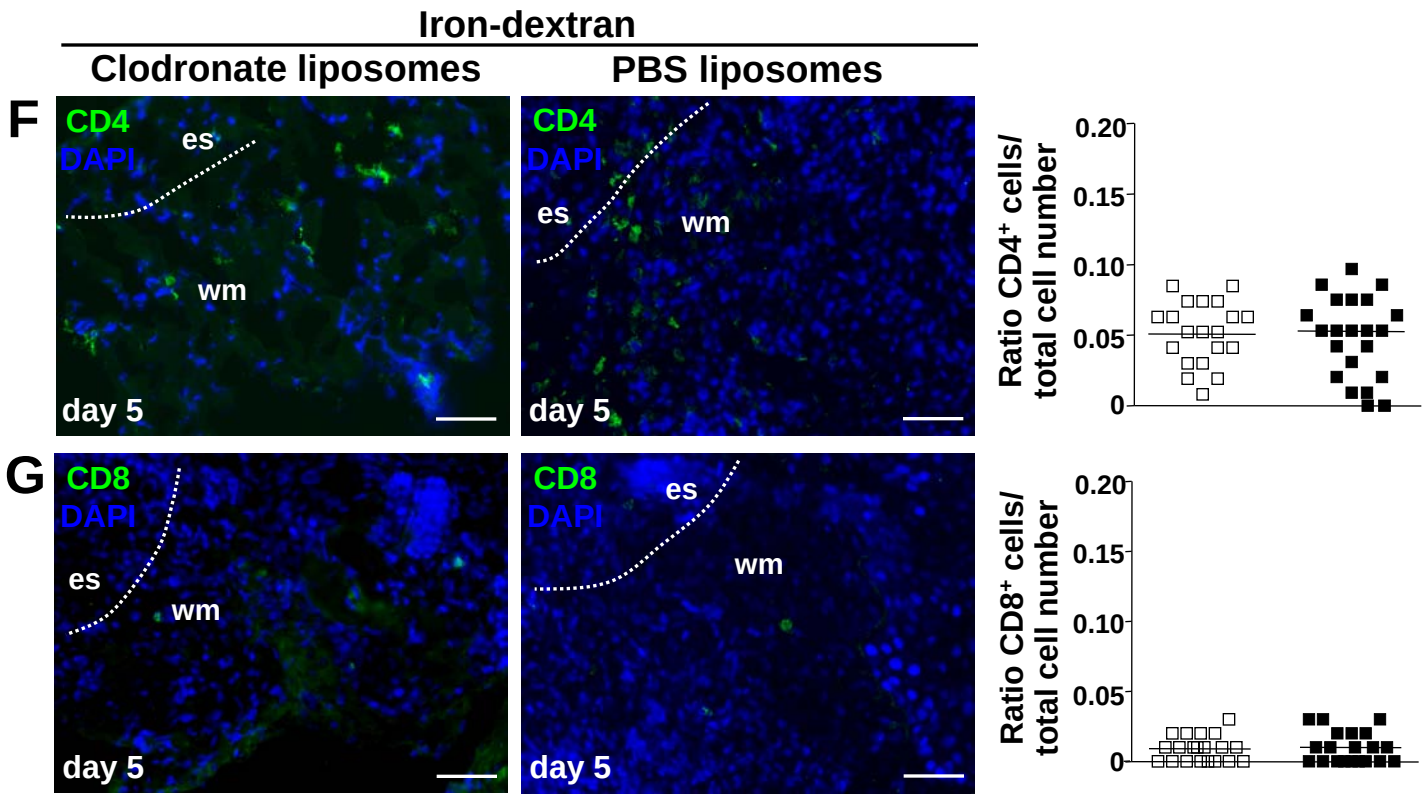

Supplemental Figure 7

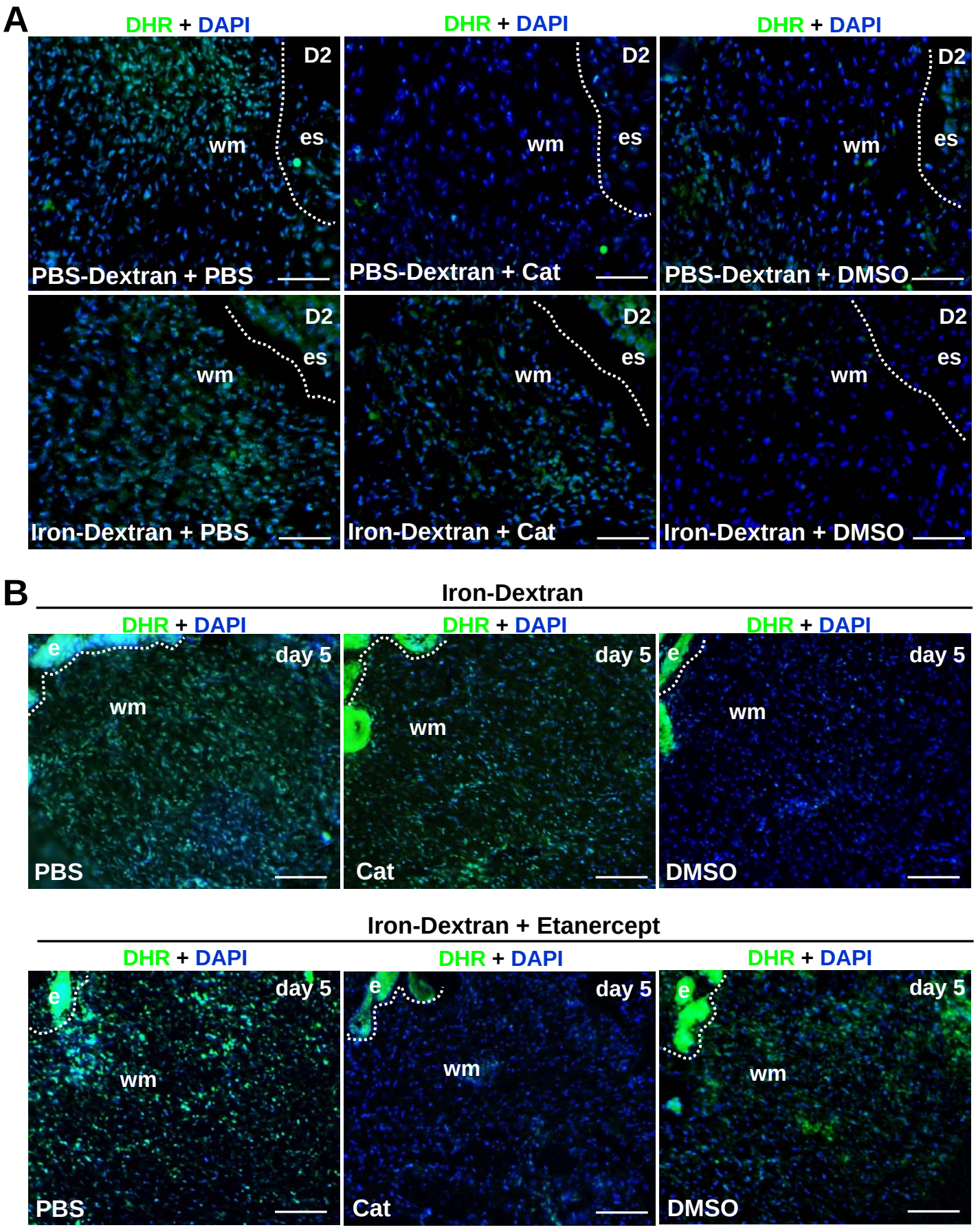

Supplemental Figure 8

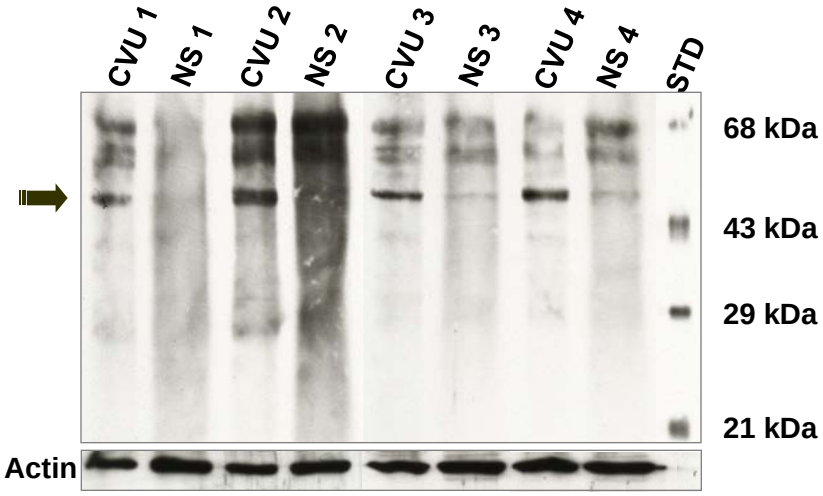

Supplemental Figure 9